PROCEEDINGS OF SCIENCE

X-ray polarization of Blazars

Luigi Costamante[a,*]

[a] *ASI - Italian Space Agency,*
Via del Politecnico snc, 00133 Rome, Italy

E-mail: luigi.costamante@asi.it

Polarization carries information about the geometry and structure of the magnetic field in blazars jets, as seen by the emitting particles. So far such studies were possible only at radio to optical frequencies. With the advent of IXPE, it is now possible to measure linear polarization in the X-ray band for several type of blazars. In high-energy-peaked blazars the X-ray band is fully dominated by the synchrotron emission of freshly accelerated electrons. Since X-ray electrons cool much faster then optical electrons, IXPE is probing the structure of the magnetic field on smaller scales and closer to the acceleration sites. Here I give an overview of the first IXPE observations of blazars, discussing the results in the context of their SED.

Multifrequency Behaviour of High Energy Cosmic Sources XIV (MULTIF2023)
12-17 June 2023
Palermo, Italy

*Speaker

PoS(MULTIF2023)035

1. Introduction

Blazars are active galactic nuclei (AGN) that produce relativistic jets of plasma, which are seen from Earth at close angle to the jet axis. Their emission is therefore boosted by relativistic beaming and dominates their entire spectral energy distribution (SED). In blazar jets, particles (electrons and possibly protons) are accelerated up to very high energies and emit by several possible mechanism, synchrotron as well as inverse Compton (IC) on seed photons of different origin, such as the same self-produced synchrotron photons (SSC mechanism) or external to the jet (EC), for example from the broad line region or infrared torus (see e.g. [1, 2]).

The resulting shape of the SED is formed by two main humps, at low and high energies. The first hump peaks between IR and X-ray energies and is ascribed to synchrotron emission from a population of relativistic electrons, since it is most often polarized. The origin of the second hump is still debated, though it is commonly attributed to inverse Compton scattering of target photons by the same electrons, and peaks in gamma-rays at MeV to TeV energies. The two peaks are correlated, forming a continuous sequence of SED shapes [3, 4], from low-energy to high-energy peaked objects (LSP to HSP), with intermediate sources (ISP) characterized by the X-ray band witnessing the transition between the two emission components [5].

The mechanism of the particle acceleration is still unclear (see e.g. [6] for a review), with the two main suspects being shocks (internal and/or standing, through diffusive shock acceleration) or magnetic reconnection. Polarimetric measurements carry information about the geometry and structure of the magnetic field seen by the emitting particles, but so far they have been limited to low energies, from radio to optical bands. With the advent of the Imaging X-ray Polarimetry Explorer (IXPE, [7]), measurements of linear polarization at X-ray energies have become possible in blazars. This is particularly important in HSP objects, where the X-ray band is fully dominated by synchrotron emission of high-energy electrons, which cool faster and thus carry information on the structure of the magnetic field close to the acceleration site.

2. Polarization mechanisms in blazars

In fully ordered magnetic fields, synchrotron emission can be polarized up to ~70-75% for electron indexes $p = 2 - 3$ [10], with relativistic aberrations slightly reducing it. In more realistic setups for shocks in blazars, the polarization degree or fraction Π_X is expected to range from a few up to ~50% (see e.g. [11]). In turbulent blazar models, where turbulence is modeled as an assembly of many small cells inside which physical parameters are uniform but can assume different values (e.g. [12]), polarization properties are expected to vary and the polarization degree to increase with frequency, depending on the number of cells contributing to the emission at a given time and energy. Polarization measurements can then provide constraints also on the scale of turbulence, depending on the observed values (reaching the maximum if only a single cell dominates the emission).

In term of properties of the electron distribution, in HSP sources the X-ray band corresponds to the emission of freshly accelerated electrons, beyond the synchotron peak in the SED, which is covered by the optical band in LSP objects. In the latter, polarization degrees from near zero up to ~50% have been observed in LSP sources, often around 10-20%, and thus similar values can be expected in X-rays from HSPs.

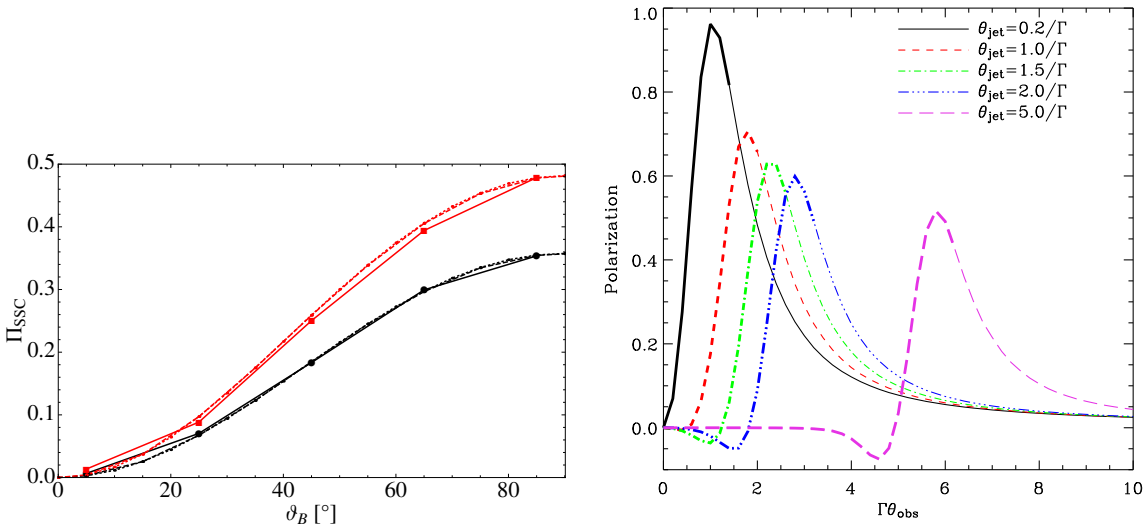

Figure 1: Left: polarization degree of the SSC emission as function of the angle between the magnetic field and the line of sight from an isotropic power-law electron population (with electron slope p and target synchrotron photon spectrum with index α), with α=1 and p=3 (squares) and α=0.5 and p=2(circles), evaluated between 10^{16} and 10^{18} Hz. Dotted lines show the predictions of an analytical approximation vs Monte Carlo simulations. From [8]. **Right:** expected polarization as a function of the observing angle in units of 1/Γ, for bulk comptonization (i.e. Compton drag) of uniform photon field. It was calculated for a relativistically-expanding fireball, but it corresponds to the case of a blazar jet for $\theta_j = 1/\Gamma$ (red line). From [9].

In LSP objects, the X-ray band corresponds instead to the low-energy part of the gamma-ray peak, and thus traces radiation from the low-energy branch of the the emitting particles distribution. If due to SSC, the mechanism is expected to reduce the polarization of the target synchrotron photons to about $\Pi_{SSC} \sim 0.1 - 0.4\ \Pi_{sync}$[8, 13–15] (see Fig. 1). Depending on the energies involved, therefore, it can go from near zero up to ∼ 20%.

Inverse Compton scattering of unpolarized seed photons, such as those produced by the torus or the broad-line region, is generally expected to produce unpolarized high-energy photons [8]. There is one very interesting exception: bulk comptonization of external photons [16]. In the jet comoving frame, any external uniform photon field is seen as beamed in a narrow cone of angle $1/\Gamma$. Thomson scattering thus gives maximum polarization for photons scattered at 90°, which is converted back in the lab frame to an angle $1/\Gamma$ from the jet axis. If electrons are cold in the comoving frame (i.e. with Lorentz factor $\gamma = 1$ to a few at most), and the geometry of the line of sight is favourable, with an angle near $1/\Gamma$ from the jet axis, bulk-motion Comptonization can then generate very high polarization levels (even up to 70-80%), because it corresponds to the emission of 90-degree Thomson-scattered photons in the jet comoving frame [9, 16]. See Fig. 1. This mechanism can easily explain very high X-ray polarization levels in flat spectrum radio sources (FSRQ), if ever observed. However, if the electrons are only moderately hot ($\gamma \geq 10$), polarization should vanish, and bulk-Compton emission might only be a transient feature lasting 1-2 days [17].

In LSP objects, the X-ray emission has also been possibly attributed to proton synchrotron, in the framework of lepto-hadronic models (e.g. [18]). In such case the emission could be more polarized,

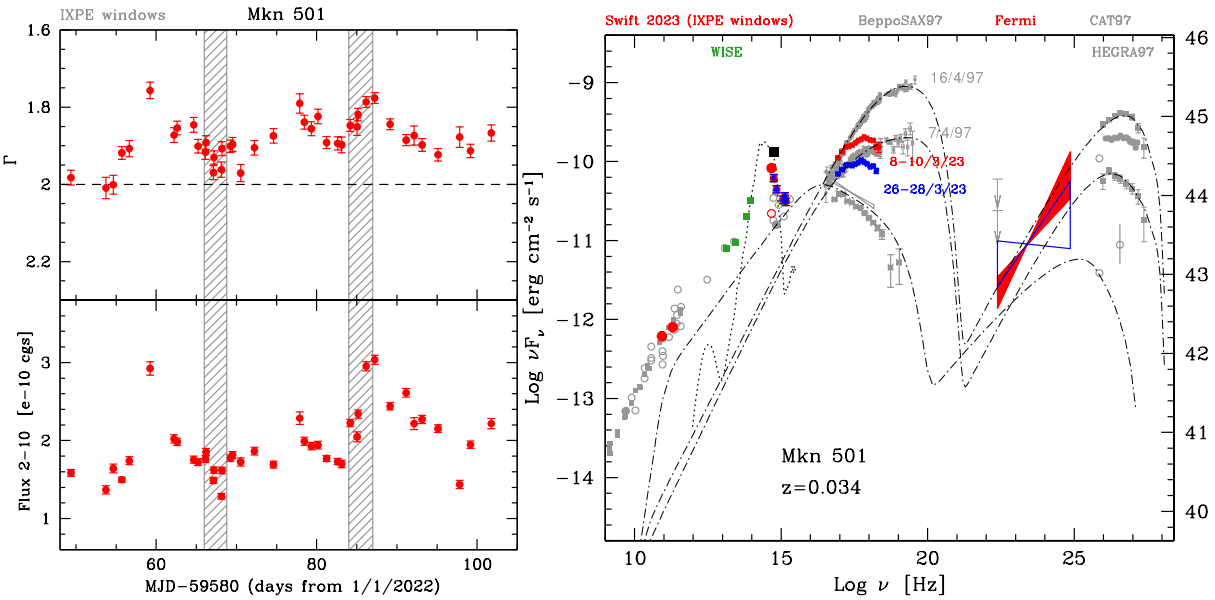

Figure 2: Left: overall lightcurve of the Swift X-ray observations in the epoch of the IXPE pointings (whose observing windows are plotted as grey bands). Upper and lower panels report the photon index Γ and 2-10 keV flux (in erg cm^{-2} s^{-1}) of the power-law fit to the XRT data. **Right:** SED of Mkn 501, with present and historical data and modeling (in grey). Red and blue points corresponds to data simultaneous to the IXPE pointings. In X-rays Mkn 501 was in a rather hard state, but not as extreme as the flaring state in 1997 or during the MAGIC campaign of 2014 [20, 21]. The synchrotron peak is constrained by the Swift data around 2-3 keV, thus the IXPE polarization measurements correspond to synchrotron emission just beyond the SED peak. The red open circle in optical corresponds to the flux level after subtraction of the host galaxy contribution. Fermi-LAT spectral data are taken from the Fermi-LAT Light curve Repository (LCR, [22]).

similarly to electron synchrotron. However, the cooling times of protons are much longer, as their energy loss rate is $(m_p/m_e)^4$ slower [19]. For protons emitting X-rays via synchrotron emission, even with B=100 Gauss the comoving coooling time would be $\sim 10^8$ s. Averaging over different magnetic field configurations could thus lead to very low polarization fractions even in the proton synchrotron scenario, at a few percent level, as it is already the case even for the electron synchrotron emission in the optical band for HSP sources.

3. IXPE results

IXPE, launched on 2021 December 9, is a joint mission of NASA and the Italian Space Agency (ASI). A description of the instrument is given by [7]. About a dozen blazars have been observed so far, of all types (HSP to LSP, BLLacs and FSRQ). Here I summarize and discuss the first results on a subset of them, with the exception of Mkn 421 which is the topic of a specific contribution in this conference (by Di Gesu et al.). The main information is summarized in Table 1. At the 30" angular resolution of IXPE, all of these sources are spatially unresolved.

In the following sections, in addition to the results from the IXPE publications, I show also the lightcurves and SED of the X-ray-polarized blazars using Swift data, whose monitoring provides an overview of the state and evolution of the objects in and around the IXPE pointings. The Swift and

SED data were analyzed as described in [23], while the Fermi-LAT results covering the IXPE windows are obtained from the Fermi-LAT Light Curve Repository (LCR, [22]), and correspond to weekly-integrated bins.

3.1 Mkn 501

The HSP BLLac Mkn 501 has been one of the first targets of IXPE [24]. X-ray polarization was expected because of its HSP nature, namely with the X-ray band fully dominated by the synchrotron emission. The fraction and angle were instead uncertain, depending on the configuration and level of ordering of the magnetic field in the emitting region.

The source has been observed 2 times at distance of ∼2 weeks, during an epoch of hard state and relative high flux, though intermediate between its range of historical X-ray spectra (see Fig. 2). Despite a factor of 2 higher flux in the first pointing, the measured values of polarization are similar, around 10% and twice higher than the optical polarization at the same epochs (after accounting for the host galaxy dilution). The overall alignment of the electric-vector position angle (EVPA) in both X-ray and optical frequencies with the jet direction observed in radio indicates that there is an overall ordered component of the magnetic field perpendicular to the jet. Similar values have been observed also in Mkn 421 (∼15% polarization, 5 times higher than in the optical [25]). The peak of the SED during the IXPE pointings, based on log-parabolic fits to the full-band XRT spectrum, can be located at 2.0 ± 0.2 keV and 3.7 ± 0.8 keV, for the 1st and 2nd pointing respectively. The curvature values are similar as well (β=0.22±0.04 and 0.23±0.04). The LAT data suggest a harder spectrum (close to $\Gamma \sim 1.5$) in the higher state.

3.2 1ES 1553+113

This HSP BLLac was observed by IXPE in February 2023 in two intervals, of 98ks and 28ks respectively [27]. The object was in a relatively low and soft X-ray state, similar to the one observed in July 2006 with Suzaku [26]. The IXPE pointings occurred in a dip of the long-term lightcurve of this source, about 200 days after a long-duration hard state in 2022, and just before a 3x increased state occurred in 2023 (see Fig. 3).

IXPE detected an average X-ray polarization degree of ∼10±2% with an electric-vector position angle ψ_X=86±8°. The detection is mainly provided by the first time interval, with Π_X=11.6±3.4% and ψ_X=85±8°. No detection is observed in the second interval (Π_X<26% at 99% confidence level), likely due to the shorter exposure time since the integrated 2-8 keV fluxes are very similar (2.47±0.03 vs 2.44±0.05 $\times 10^{-11}$ erg cm^{-2} s^{-1}).

Quite interestingly, in the timespan between the two intervals the optical polarization varied significantly, from 2% to 4% with a smooth rotation of the polarization angle from 0° to ∼125° which occurred with a rate of ∼17° per day [27]. Unfortunately, we cannot draw conclusions on a corresponding behaviour of the X-ray polarization: the non-detection of the 2nd interval prevent us to compare the angles between the two epochs, and the absence of evidence for a rotation of $\psi_X$inside the first interval is likely due to the low statistics (it would need to divide the interval in 2-3 shorter timebins of exposure similar to the second interval, and thus too short for a detection).

Comparing the X-ray and optical angles in the first interval, there is a difference of about $\Delta\psi$ ∼90° to 70° (see Fig. 3 in [27]), suggesting that for this source the configuration of the magnetic field seen by the optical and X-ray emitting electrons is different, and almost perpendicular.

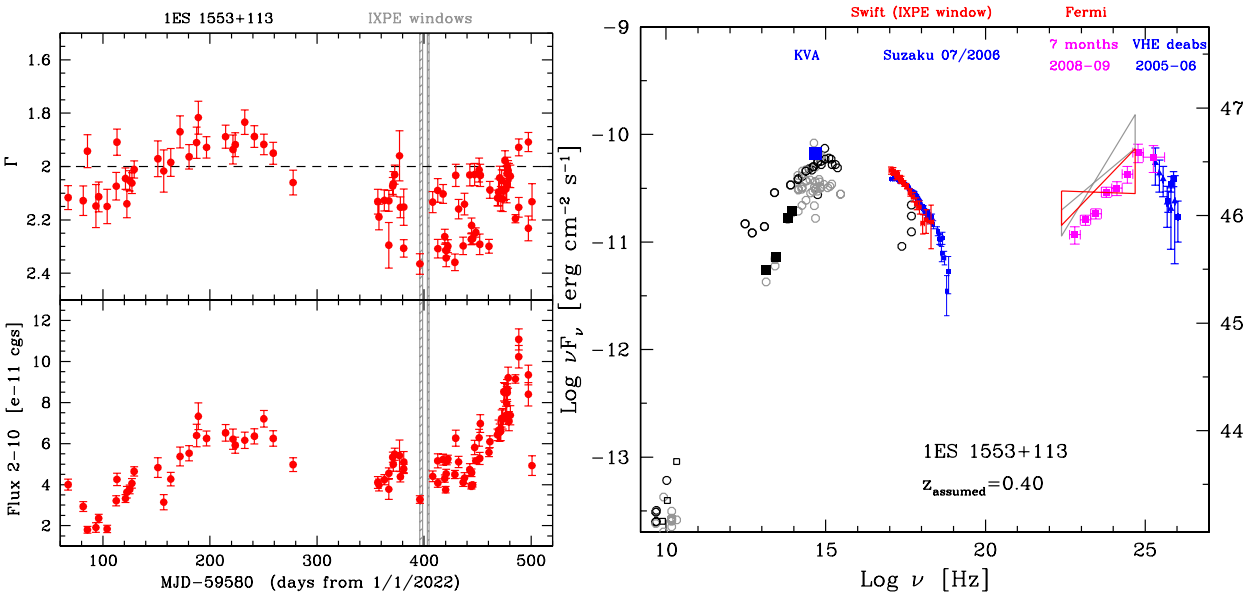

Figure 3: Left: overall lightcurve of the Swift X-ray observations in the epoch of the IXPE pointings (whose observing windows are plotted as grey bands). The source was observed during a rather low and soft state, ~200 days after a hard state and just before 3x flux increase over several weeks. **Right:** SED of 1ES 1553+113 with present and historical data (in grey and black). Red points correspond to the Swift spectrum closest to the IXPE observation. Blue data correspond to same-epoch data during the Suzaku campaign of 2006 [26], while magenta points report the Fermi-LAT spectrum of the first 7 months of observations in 2008-2009. The source was in a state similar to the 2006 spectrum, with the IXPE band sampling the synchrotron emission well beyond the synchrotron peak.

The position of the (faint) radio jet at 15 GHz, as imaged with the MOJAVE program, is at a projected position angle between 30° and 50°. The observed X-ray polarization position angle seems thus oblique to the parsec-scale jet direction, with a difference of ~45°, similar to what observed in Mkn 421 during its first IXPE observation [25]. However, the position angle of the jet in this source is known to vary over time [28].

In this object, the radio and optical polarization degrees are lower by a factor of 3 with respect to the X-ray values.

3.3 1ES 0229+200

This HSP BLLac is the prototype of the extreme-TeV BL Lac class, being characterized by a constantly hard TeV spectrum which locates its gamma-ray peak in the SED persistently above 10 TeV [23, 30]. Such high-energies are very difficult to explain with standard one-zone SSC models. They generally require extreme conditions with very low magnetic fields, several orders of magnitude below equipartition, unusually hard electron distributions and very low radiative efficiency [23, 30, 31].

1ES 0229+200 was observed by IXPE at the beginning of 2023 in two intervals, January 15-18 and from January 27 to February 1, for a total of 401 ks [32]. The pointings occurred in a low-flux phase of the typical state of this source in 2023 (see Fig. 4), but the overall variations in 2023 have been of small amplitude, within a factor of 2. IXPE has detected an average X-ray polarization

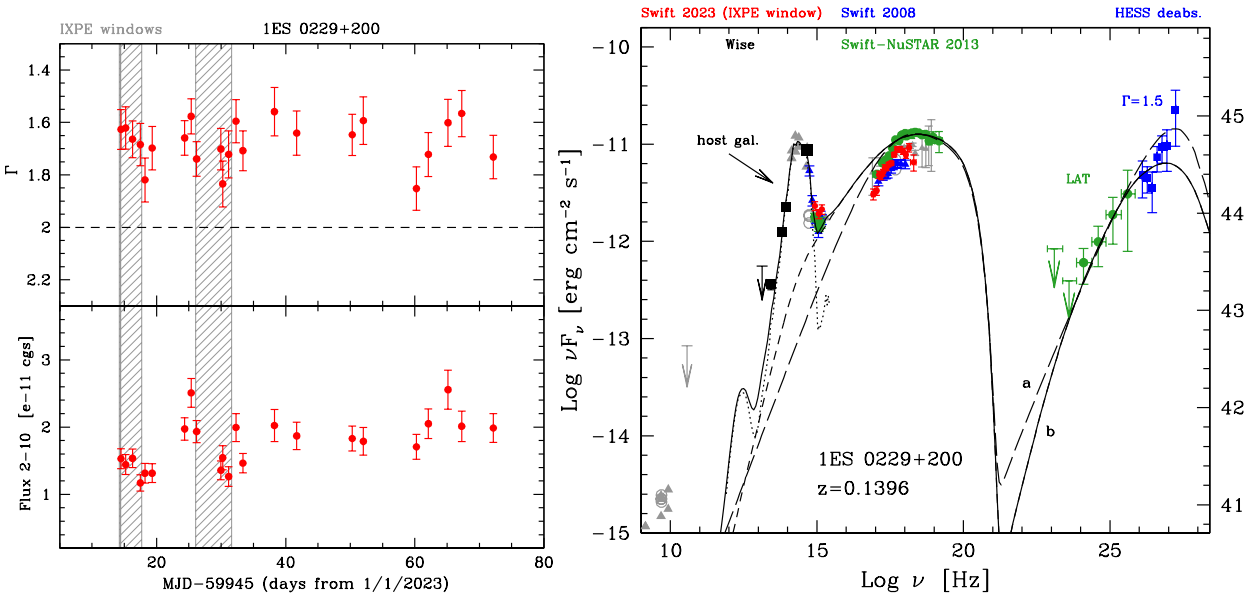

Figure 4: Left: overall lightcurve of the Swift X-ray observations in the epoch of the IXPE pointings (grey bands). The XMM-Newton observation (18ks, filled grey band) occurred at the beginning the 1st IXPE segment. The X-ray spectrum has been always hard, as characterictic of this extreme BL Lac. **Right:** SED of 1ES 0229+200 with present and historical data (in green and blue). Red points correspond to the summed Swift data simultaneous to the IXPE observation. Green points correspond to same-epoch data during the Swift-NuSTAR campaign of 2013 [23], while blue points correspond to the Swift and H.E.S.S. observations in 2005-2008 [23, 29]. The extrapolation of the X-ray spectrum at lower frequencies does not connect as a single component with the UV fluxes from UVOT, even in a clearer way than in 2013. This indicates that the optical-emitting electrons likely correpond to a different region than the X-ray electrons.

degree of ∼18±3% with an electric-vector position angle ψ_X=86±8°, from spectropolarimetric fits. No evidence for any dependence of the polarization on energy is found, as well as for a time dependence [32].

The object was too faint in Radio for a polarization measurement, with upper limits at 7%, while in Optical simultaneous observations give values of Π_O=2.4 − 3.2%±0.7%, after accounting for the host galaxy contamination, with angles between -2° and -5° [32]. Comparing the X-ray and optical angles, there is no clear relationship between the two, nor with the radio jet which has an apparent position angle of ∼160° east of north [32].

In this source therefore the X-ray polarization is more than 6-7 times higher than the optical polarization, one of the highest ratios observed so far. However, the optical emission in this object seems to belong to a completely different component with respect to the X-ray emission. In fact the slope of the soft X-ray spectrum as measured by Swift does not allow a smooth connection with the UV flux from UVOT, which have negligible contamination by the thermal emission of the elliptical host galaxy at these frequencies (see Fig. 4). Note that this is not an effect of the uncertainty on the value of galactic N_H: for the spectral fit in Fig. 4 I have used the value of N_H=9.21×10^{20} cm^{-2} from Dickey & Lockman [33], which is the highest among the recent estimates. Lower values like N_H=7.82×10^{20} cm^{-2} from the more recent maps by the HI4PI Collaboration [34] would make the spectrum even harder, in this case by $\Delta\Gamma$ = 0.03, worsening the tension with the UV flux.

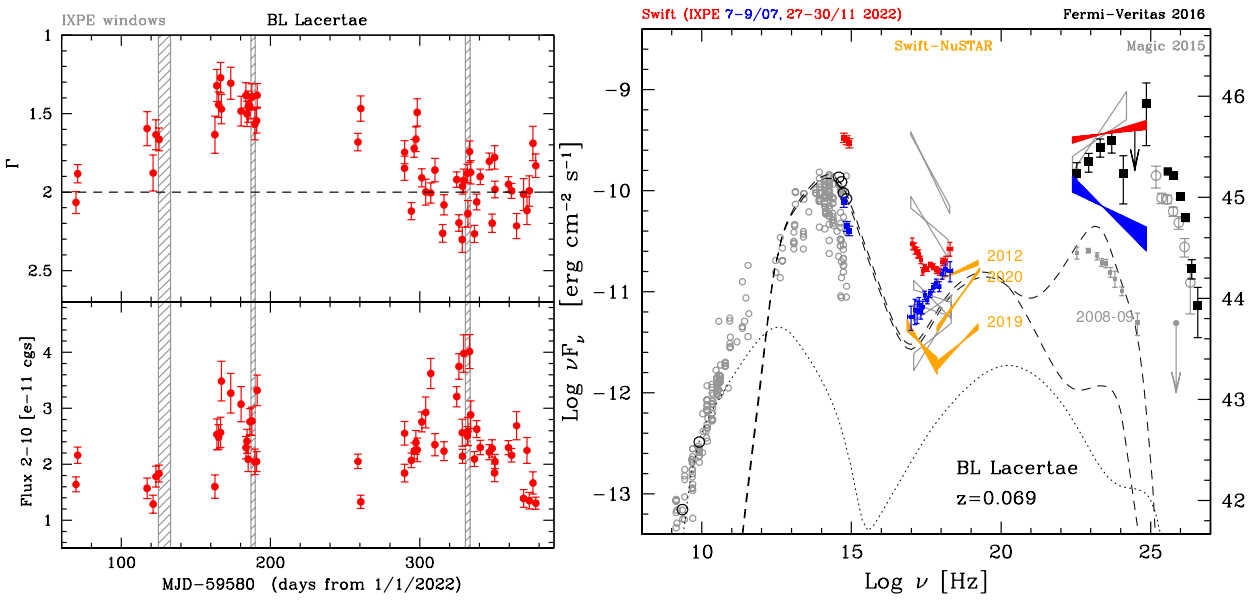

Figure 5: Left: overall lightcurve of the Swift X-ray observations in the epoch of the IXPE pointings (whose observing windows are plotted as grey bands). **Right:** SED of BL Lac, with present and historical data and modeling (in grey/black). Recent historical Swift and Swift-NuSTAR observations in 2012-2020 are plotted in orange. Blue and red points correspond to data during the 2nd and 3rd IXPE pointings, respectively. In the 2nd observation (blue points) BL Lac was in a clear LSP state, with the whole 0.3-10 keV band dominated by IC emission and a steep Fermi-LAT spectrum locating the gamma-ray peak below 100 MeV. In the 3rd observation, instead, BL Lac was in an ISP state (red points), with the soft X-ray band dominated by the tail of the synchrotron emission, which extended into the 2-4 keV band in the first time bin of the IXPE pointing, yielding the polarization detection and a steep spectrum in IXPE [35]. The harder and higher electron spectrum leads to a hardening of the Fermi-LAT spectrum as well, yielding a gamma-ray peak likely beyond 10 GeV, similarly to HSPs.

The peak of the SED during the IXPE pointings, based on log-parabolic fits to the average full-band XRT spectrum simultaneous to the IXPE pointings, can be located at $4.3 - 1.1 + 3.2$ keV, with curvature value β=0.38±0.14. Note however that these high values of curvature might be caused in part by the degradation of the XRT CCD, not yet fully corrected for recent observations with the present RMF and ARF calibration. These will be updated soon in an upcoming CALDB release at the end of this year, so these values must be considered at present preliminary. The spectral index reported in Table 1 is obtained from the XMM-Newton observation, which took place at the very beginning of the IXPE first segment. In such case the peak can be located at ∼25 keV, with curvature β=0.13±0.02 and a corresponding slope at 4 keV of $\Gamma = 1.9$ [32].

3.4 BL Lacertae

BL Lacertae gave the name to this class of blazars, and SED-wise it is in general an object of LSP type, thus with the X-ray band usually dominated by the IC emission of low-energy electrons. However, it is known to undergo active states when the electrons are accelerated to much higher energies, yielding a harder synchrotron emission which enters in the soft X-ray band, as typical for ISP objects, or even dominating it up to ∼10 keV [36, 37]. Such states are also accompanied by

enhanced flux in GeV gamma-rays and at VHE.

IXPE observed this object 3 times in 2022 (see Fig. 5). In the first two pointings the object was generally in a low-flux and hard state, as typical of a LSP SED. During these observations, no polarization detection was achieved, with an upper limit of $\Pi_X < 12.6\%$ at 99% confidence level [38]. In this case, the simultaneous optical polarization fraction reached values higher than the X-rays upper limits, at Π_O=14.2%.

Things changed in the third pointing [35]. BL Lacertae was observed in an active state, with a softer X-ray spectrum indicating the possible presence of the high-energy tail of the synchrotron emission entering in the soft-X-ray. Indeed this becomes clear in the SED with the Swift spectrum (see Fig. 5), which shows the characteristic concave shape typical of ISP blazars. A fit of the combined NuSTAR, XMM and IXPE same-epoch spectra with the sum of two power-laws constrains the soft (synchrotron) slope to $\Gamma_1 = 3.3 \pm 0.1$ [35]. Dividing the IXPE interval in 3 timebins, in the time bin with highest estimated synchrotron flux contribution a detection of X-ray polarization was found in the 2-4 keV band at > 99% confidence level, with Π_X= 21.7+5.6−7.9% and ψ_X=-29±9°. This polarization is ∼2× higher than the simultaneous optical polarization Π_O=13.1±2.4% for the same time bin [35].

From the analysis of the hard X-ray spectrum, the IC emission is still expected to contribute for about 56% of the total flux in the 2-4 keV band. Depending on the assumption on its origin and polarization degree (i.e. if SSC polarized at ∼0.3× the synchrotron value or if unpolarized IC), the actual polarization of the synchrotron component could be as high as 36% or 49%, respectively [35].

Concerning polarization angles, both the optical and X-ray EVPA are similar and at ∼40° to the projection of the jet axis on the plane of the sky at 43GHz [35].

Also in gamma-rays the hardening of the emission is evident: the Fermi-LAT spectrum is significantly harder than in the previous pointing, indicating a shift of the gamma-ray peak in the SED from <100 MeV to near or beyond 10 GeV.

3.5 LSP blazars

Together with BL Lacertae, IXPE has observed other LSP blazars in 2022-2023. In particular, the well known 3C 273, S5 0716+714 and the two bright FSRQs 3C 279 and 3C 454.3.

The IXPE polarimetric data were studied with an unbinned event-based likelihood analysis [39], that accounts for the background. No clear detections of X-ray polarization are observed in any of these objects. The 99% confidence limits range from 9% to 28% [40] (see Table 1). As shown in the case of Mkn 421 [41], rotations of the EVPA during observations, especially for exposures longer than the typical variability timescales (∼1-2 days) in blazars, can lead to depolarization. Testing with the same method described in [41], using an event-based likelihood [39], no evidence for EVPA rotations was found in any of the four sources [40].

S5 0716+714 is usually a highly variable source with large outbursts yielding detections also at VHE. In optical, the polarization during the IXPE pointing varied significantly between 1 and 13%. In X-rays however the flux was particularly low, so that only an upper limit of 26% is obtained despite the long exposure (358ks). The spectral data indicate that this source was likely in an ISP state, which could lead to detection of significant polarization with slightly harder flares in the synchotron emission.

Source	date	exp.	Γ_X	Π_X	ψ_X	Π_O	ψ_O	refs
Mkn 501	9-10/3/22	100ks	2.20±0.05	10±2%	134±5°	4±1%	119±9°	[24]
	26-28/3/22	86ks	2.07±0.05	11±2%	115±4°	5±1%	117±3°	[24]
1ES 1553+113	1-3,8-9/2/23	126ks	2.59±0.03	10±2%	86±8°	2-4±0.5%	0-125°	[27]
1ES 0229+200	15/1—1/2/23	401ks	1.90±0.01	18±3%	25±5°	2-4±0.7%	-2±9°	[32]
BL Lacertae	27-30/11/22	287ks	3.28±0.10	22±8%	-29±9°	6-17±0.3%	-20-0°	[35]
BL Lacertae	6-14/5/22	390ks	1.74±0.01	<14.2%	-	6.8%	~107°	[38]
	9-11/7/22	116ks	1.87±0.06	<12.6%	-	14.2%	~42°	[38]
S5 0716+714	31/3-5/4/22	358ks	2.29±0.20	< 26%	-	1-13%	~5-100°	[40]
3C 279	13-18/6/22	264ks	1.79±0.04	< 12.7%	-	12%	~175-165°	[40]
3C 273	2-4/6/22	95ks	1.80±0.02	< 9.0%	-	<0.5%	-	[40]
3C 454.3	31/5-2/6/22	98ks	1.71±0.08	< 28%	-	<1%	-	[40]

Table 1: Summary of the main polarization and spectral measurements during the IXPE pointings. Full information in the respective references (last column). Date, exposure and X-ray polarization values (polarization fraction and EVPA) are from the IXPE data. Optical values correspond to the average values (or range of variations) during the IXPE pointings, taken from various ground-based telescopes (as detailed in each reference). Values of the X-ray photon index Γ_X are from combined fits of the IXPE spectrum with other X-ray satellites (either the index of the power-law fit, or the index of the log-parabolic fit at 4 keV), except for Mkn 501, where the values are from power-law fits of the summed Swift data simultaneous to the IXPE pointings, limited to the 2-10 keV range. The upper box reports sources/states where the X-ray band is dominated by synchrotron emission. The lower box reports sources/states dominated by inverse Compton emission, as shown by the photon index. The values of the BL Lacertae entry in the upper box (3rd IXPE observation of November 2022) reports the measurements of the polarization detection, i.e. limited to the 2-4 keV band and first time bin of the IXPE observation, when the 2-4 keV band was dominated by the tail of the synchrotron hump (see [35]).

3C 454.3 has been one of the brightest FSRQs in the Fermi era, both in X-rays and gamma-rays. It is well known for huge outbursts especially in optical and gamma-rays, i.e. close to the two peaks of the SED. In optical, when this band becomes dominated by the jet emission over the thermal disk emission, polarization can reach values as high as 30% [42]. During these first IXPE observations however, the optical polarization was below 1%, with a stable EVPA within the uncertainties. Also in mm-radio wavebands, only upper limits at 1-3% were obtained [40].

4. Discussion

This first set of IXPE measurements of X-ray polarization in blazars have provided us with some new information on the structure of the magnetic field in the emitting region of blazars jets, close to the acceleration sites.

So far detections have been obtained only for the synchrotron emission. The results on HSP blazars such as Mkn 501, 1ES 1553+113 and 1ES 0229+200 (as well as Mkn 421, [25]) indicate that the polarization in X-rays at or beyond the SED peak is at 10-18%, about 2-7× higher than at optical frequencies. Under the assumption of belonging to the same dissipation event or region, this might be due to energy-stratified shocks, where electrons accelerated at the shock front emit X-ray synchrotron radiation only in a thin layer close to the shock front, thus experiencing a more ordered magnetic field. Beyond that layer the maximum electron energy decreases due to radiative

cooling, reducing the X-ray emission but not the optical emission, which is emitted by longer-lived lower-energy electrons. The wider volume contributing to the optical emission thus reduces the overall polarization signal [24].

However, it must be noted that this is a more general argument, not specific to energy-stratified shocks. In addition, the larger depolarization at optical frequencies can have other origins. For example, a completely different zone with a less-ordered configuration of the magnetic field or with different turbulence levels, even if the actual sizes of the X-ray and optical regions were comparable. Another possibility is that the flux in optical is the sum of the emission from more than one knot/zone in the jet (see e.g the optical knots in M87), since electrons require less acceleration to reach optical energies and live longer than for X-ray energies.

In fact, it is not clear if optical and X-ray emissions actually come from the same dissipation region. For some HSPs like 1ES 0229+200 the X-ray spectrum does not connect consistently with the optical emission, and thus do not seem to belong to the same emitting component (see Fig. 4 and [23]). This could also be the reason of the different EVPA observed in 1ES 1553+113 between optical and X-ray energies. Indeed, also the rotation of ψ_X seen in Mkn 421 not accompanied by a similar behaviour in optical [41] supports this possibility, somewhat undermining the assumption at the basis of the conclusion for energy-stratified shocks.

More generally, the IXPE results are just telling that B seems more ordered in the region of the X-ray emission rather than the optical emission. Optical synchotron photons are produced by ~50× less energetic electrons than X-rays photons (at 3-4 keV), thus these electrons cool in 50× longer timescales and over regions that can be up to 50× larger in size. This argument works also in case of turbulence [43], as long as the scale of the cells where B is locally ordered remains smaller than the emitting regions. In this scenario, smaller emitting regions (coming from a lower number of active cells as can occur in fast variability events) should yield higher mean polarization and more strongly variable, possibly in a random manner if B is randomly distributed among cells. This can be tested in future observations of flaring events.

In this respect, quite interesting is the possibility of very high polarization in the highest-energy tail of the synchrotron emission seen in BL Lacertae, where it could have reached 30-50%. It will be important to obtain X-ray polarization measurements in large flaring events like Mkn 501 in 1997, where fast variability coupled with large fluxes can allow us to investigate in detail the structure of B at smaller scales during both acceleration and dissipation phases.

Concerning angles, no common trend has emerged so far in the orientation of the magnetic field derived in X-ray with respect to optical frequencies, or to the radio jet. Different sources seem to have different configurations (e.g. similar to the optical orientation and perpendicular to the radio jet in Mkn 501, while different and oblique in 1ES 1553+113). Likewise for the rotation of the polarization angles, which has not been observed so far occurring at X-ray and optical frequencies at the same time (with possibly opposite behaviours in Mkn 421 with respect to 1ES 1553+113 [27, 41]).

No polarization detection has been observed so far for the IC emission in LSP, regardless of its origin. However, the obtained upper limits are still too high to draw any conclusion. The generally low polarization levels are expected even in the SSC case, given the observed levels of synchrotron polarization. Also the scenario of proton synchrotron emission cannot be disfavoured, since at these energies, even with B~100 Gauss the cooling time of protons emitting X-ray electrons is very long,

and thus by averaging over different B orientations the overall polarization might be very low (as is the case for optical electrons in HSPs, for example). Bulk comptonization of external photons might produce very high polarization, but the peculiar observation angles required and possibly transient nature of such emission limit its chance of detectability. To test X-ray polarization in LSPs it is necessary to go down to a few percent in MDP, and to observe during peculiar source states in order to catch bulk comptonization events.

The X-ray band in LSPs is quite crowded in terms of emission components, for the possible (even simultaneous) presence of emission from very different mechanisms such as SSC, EC, proton synchrotron or photo-meson production, or bulk comptonization components. For the proton-synchrotron origin of the high-energy hump in blazars' SED, more clear answers might come from the upcoming COmpton Spectrometer and Imager mission (COSI, [44]), which can test gamma-ray polarization at MeV energies for the brightest sources.

Acknowledgments

I wish to thank the organizers for their kind invitation to give this overview, and for the usual excellent hospitality. I thank H. Marshall, S. Ehlert and the IXPE team for anticipating some results. This research has used publications and results of the IXPE Team (MSFC, ASI-SSDC, INAF, and INFN) and Swift data and analysis software distributed by the High-Energy Astrophysics Science Archive Research Center (HEASARC), with XRT Data Analysis Software (XRT-DAS) developed under the responsibility of the ASI Space Science Data Center (SSDC).

References

[1] G. Ghisellini and F. Tavecchio, *Canonical high-power blazars*, MNRAS **397** (2009) 985 [0902.0793].

[2] M. Sikora, Ł. Stawarz, R. Moderski, K. Nalewajko and G. M. Madejski, *Constraining Emission Models of Luminous Blazar Sources*, ApJ **704** (2009) 38 [0904.1414].

[3] P. Padovani and P. Giommi, *The connection between x-ray- and radio-selected BL Lacertae objects*, ApJ **444** (1995) 567 [astro-ph/9412073].

[4] G. Ghisellini, C. Righi, L. Costamante and F. Tavecchio, *The Fermi blazar sequence*, MNRAS **469** (2017) 255 [1702.02571].

[5] G. Tagliaferri, G. Ghisellini, P. Giommi, L. Chiappetti, L. Maraschi, A. Celotti et al., *The concave X-ray spectrum of the blazar ON 231: the signature of intermediate BL Lacertae objects*, A&A **354** (2000) 431 [astro-ph/9912055].

[6] J. H. Matthews, A. R. Bell and K. M. Blundell, *Particle acceleration in astrophysical jets*, New A Rev. **89** (2020) 101543 [2003.06587].

[7] M. C. Weisskopf, P. Soffitta, L. Baldini, B. D. Ramsey, S. L. O'Dell, R. W. Romani et al., *The Imaging X-Ray Polarimetry Explorer (IXPE): Pre-Launch*,

Journal of Astronomical Telescopes, Instruments, and Systems **8** (2022) 026002 [2112.01269].

[8] H. Krawczynski, *The Polarization Properties of Inverse Compton Emission and Implications for Blazar Observations with the GEMS X-Ray Polarimeter*, ApJ **744** (2012) 30 [1109.2186].

[9] D. Lazzati, E. Rossi, G. Ghisellini and M. J. Rees, *Compton drag as a mechanism for very high linear polarization in gamma-ray bursts*, MNRAS **347** (2004) L1 [astro-ph/0309038].

[10] G. B. Rybicki and A. P. Lightman, *Radiative processes in astrophysics*. 1979.

[11] F. Tavecchio, *Probing Magnetic Fields and Acceleration Mechanisms in Blazar Jets with X-ray Polarimetry*, *Galaxies* **9** (2021) 37 [2105.08401].

[12] A. P. Marscher, *Turbulent, Extreme Multi-zone Model for Simulating Flux and Polarization Variability in Blazars*, ApJ **780** (2014) 87 [1311.7665].

[13] J. Poutanen, *Relativistic Jets in Blazars: Polarization of Radiation*, ApJS **92** (1994) 607.

[14] A. L. Peirson and R. W. Romani, *The Polarization Behavior of Relativistic Synchrotron Self-Compton Jets*, ApJ **885** (2019) 76 [1909.10563].

[15] A. L. Peirson, I. Liodakis and R. W. Romani, *Testing High-energy Emission Models for Blazars with X-Ray Polarimetry*, ApJ **931** (2022) 59 [2204.11803].

[16] M. C. Begelman and M. Sikora, *Inverse Compton Scattering of Ambient Radiation by a Cold Relativistic Jet: A Source of Beamed, Polarized X-Ray and Optical Observations of X-Ray–selected BL Lacertae Objects*, ApJ **322** (1987) 650.

[17] A. Celotti, G. Ghisellini and A. C. Fabian, *Bulk Comptonization spectra in blazars*, MNRAS **375** (2007) 417 [astro-ph/0611439].

[18] H. Zhang and M. Böttcher, *X-Ray and Gamma-Ray Polarization in Leptonic and Hadronic Jet Models of Blazars*, ApJ **774** (2013) 18 [1307.4187].

[19] F. A. Aharonian, *Very high energy cosmic gamma radiation : a crucial window on the extreme Universe*. 2004, 10.1142/4657.

[20] E. Pian, G. Vacanti, G. Tagliaferri, G. Ghisellini, L. Maraschi, A. Treves et al., *BeppoSAX Observations of Unprecedented Synchrotron Activity in the BL Lacertae Object Markarian 501*, ApJ **492** (1998) L17 [astro-ph/9710331].

[21] MAGIC Collaboration, V. A. Acciari, S. Ansoldi, L. A. Antonelli, A. Babić, B. Banerjee et al., *Study of the variable broadband emission of Markarian 501 during the most extreme Swift X-ray activity*, A&A **637** (2020) A86 [2001.07729].

[22] S. Abdollahi, M. Ajello, L. Baldini, J. Ballet, D. Bastieri, J. Becerra Gonzalez et al., *The Fermi-LAT Lightcurve Repository*, ApJS **265** (2023) 31 [2301.01607].

[23] L. Costamante, G. Bonnoli, F. Tavecchio, G. Ghisellini, G. Tagliaferri and D. Khangulyan, *The NuSTAR view on hard-TeV BL Lacs*, MNRAS **477** (2018) 4257 [1711.06282].

[24] I. Liodakis, A. P. Marscher, I. Agudo, A. V. Berdyugin, M. I. Bernardos, G. Bonnoli et al., *Polarized blazar X-rays imply particle acceleration in shocks*, Nature **611** (2022) 677 [2209.06227].

[25] L. Di Gesu, I. Donnarumma, F. Tavecchio, I. Agudo, T. Barnounin, N. Cibrario et al., *The X-Ray Polarization View of Mrk 421 in an Average Flux State as Observed by the Imaging X-Ray Polarimetry Explorer*, ApJ **938** (2022) L7 [2209.07184].

[26] A. Reimer, L. Costamante, G. Madejski, O. Reimer and D. Dorner, *A Hard X-Ray View of Two Distant VHE Blazars: 1ES 1101-232 and 1ES 1553+113*, ApJ **682** (2008) 775 [0808.0184].

[27] R. Middei, M. Perri, S. Puccetti, I. Liodakis, L. Di Gesu, A. P. Marscher et al., *IXPE and Multiwavelength Observations of Blazar PG 1553+113 Reveal an Orphan Optical Polarization Swing*, ApJ **953** (2023) L28 [2308.00039].

[28] R. Lico, J. Liu, M. Giroletti, M. Orienti, J. L. Gómez, B. G. Piner et al., *A parsec-scale wobbling jet in the high-synchrotron peaked blazar PG 1553+113*, A&A **634** (2020) A87 [2001.01753].

[29] F. Aharonian, A. G. Akhperjanian, U. Barres de Almeida, A. R. Bazer-Bachi, B. Behera, M. Beilicke et al., *New constraints on the mid-IR EBL from the HESS discovery of VHE γ-rays from 1ES 0229+200*, A&A **475** (2007) L9 [0709.4584].

[30] J. Biteau, E. Prandini, L. Costamante, M. Lemoine, P. Padovani, E. Pueschel et al., *Progress in unveiling extreme particle acceleration in persistent astrophysical jets*, *Nature Astronomy* **4** (2020) 124 [2001.09222].

[31] A. Zech and M. Lemoine, *Electron-proton co-acceleration on relativistic shocks in extreme-TeV blazars*, A&A **654** (2021) A96 [2108.12271].

[32] S. R. Ehlert, I. Liodakis, R. Middei, A. P. Marscher, F. Tavecchio, I. Agudo et al., *X-ray Polarization of the BL Lac Type Blazar 1ES 0229+200*, *arXiv e-prints* (2023) arXiv:2310.01635 [2310.01635].

[33] J. M. Dickey and F. J. Lockman, *H I in the galaxy.*, ARA&A **28** (1990) 215.

[34] HI4PI Collaboration, N. Ben Bekhti, L. Flöer, R. Keller, J. Kerp, D. Lenz et al., *HI4PI: A full-sky H I survey based on EBHIS and GASS*, A&A **594** (2016) A116 [1610.06175].

[35] A. L. Peirson, M. Negro, I. Liodakis, R. Middei, D. E. Kim, A. P. Marscher et al., *X-Ray Polarization of BL Lacertae in Outburst*, ApJ **948** (2023) L25 [2305.13898].

[36] M. Ravasio, G. Tagliaferri, G. Ghisellini, P. Giommi, R. Nesci, E. Massaro et al., *BL Lacertae: Complex spectral variability and rapid synchrotron flare detected with BeppoSAX*, A&A **383** (2002) 763 [astro-ph/0201307].

[37] M. Ravasio, G. Tagliaferri, G. Ghisellini, F. Tavecchio, M. Böttcher and M. Sikora, *BeppoSAX and multiwavelength observations of BL Lacertae in 2000*, A&A **408** (2003) 479 [astro-ph/0307021].

[38] R. Middei, I. Liodakis, M. Perri, S. Puccetti, E. Cavazzuti, L. Di Gesu et al., *X-Ray Polarization Observations of BL Lacertae*, ApJ **942** (2023) L10 [2211.13764].

[39] H. L. Marshall, *Multiband Weighting of X-Ray Polarization Data*, ApJ **907** (2021) 82 [2012.01283].

[40] H. L. Marshall, I. Liodakis, A. P. Marscher, N. Di Lalla, S. G. Jorstad, D. E. Kim et al., *Observations of Low and Intermediate Spectral Peak Blazars with the Imaging X-ray Polarimetry Explorer*, *arXiv e-prints* (2023) arXiv:2310.11510 [2310.11510].

[41] L. Di Gesu, H. L. Marshall, S. R. Ehlert, D. E. Kim, I. Donnarumma, F. Tavecchio et al., *Discovery of X-ray polarization angle rotation in the jet from blazar Mrk 421*, *Nature Astronomy* (2023) [2305.13497].

[42] I. Liodakis, D. Blinov, S. G. Jorstad, A. A. Arkharov, A. Di Paola, N. V. Efimova et al., *Two Flares with One Shock: The Interesting Case of 3C 454.3*, ApJ **902** (2020) 61 [2008.08603].

[43] A. P. Marscher and S. G. Jorstad, *Linear Polarization Signatures of Particle Acceleration in High-Synchrotron-Peak Blazars*, *Universe* **8** (2022) 644.

[44] J. A. Tomsick, S. E. Boggs, A. Zoglauer, D. Hartmann, M. Ajello, E. Burns et al., *The Compton Spectrometer and Imager*, *arXiv e-prints* (2023) arXiv:2308.12362 [2308.12362].